Hydrothermal Synthesis of Manganese Sulfide Decorated Graphene Oxide for Effective Electrochemical Sensing of Dopamine

Settu Ramki[1], Karuppaih Pandi[1], Shen-Ming Chen[*1], Yi-Ting Ye[1], Tse-Wei Chen[1], Qingli Hao[*2]

[1]Electroanalysis and Bioelectrochemistry Lab, Department of Chemical Engineering and Biotechnology, National Taipei University of Technology, Taipei 10608, Taiwan.
[2]Key Laboratory for Soft Chemistry and Functional Materials, NanjingUniversity of Science and Technology, Ministry of Education, Nanjing,China.
[*]E-mail: smchen78@ms15.hinet.net (Shen-Ming Chen) ; haoqingli@yahoo.com (Qingli Hao)

Microsphere like structured manganese sulfide decorated graphene oxide (MnS/GO) composites were synthesized by using simple hydrothermal method. The above prepared MnS/GO composite was characterized by using X-ray diffraction spectroscopy (XRD), Scanning Electron Microscopy (SEM), Energy Dispersive X-ray analysis (EDX), and Raman spectroscopy. The obtained results confirmed the formation of MnS/GO composite with required stoichiometry and morphology. For the first time, MnS based materials were used as a modifier and dopamine as a model system for the electrochemical application. The electrochemical studies were performed for MnS/GO composite modified GCE using Cyclic Voltammetry (CV) and linear sweep voltammetry techniques. The results suggest that the effective response of MnS/GO/GCE with very low limit of detection (LOD) and sensitivity of 0.007 μM and 3.11 μA μM^{-1}cm^{-2} respectively. Moreover the selectivity results exhibited excellent interference property of MnS/GO/GCE towards sensing of dopamine. Moreover, the reported MnS/GO/GCE sensor exhibits excellent long cyclic stability, and selectivity and greater support for the real-time detection of DA in human urine samples. Thus, the proposed MnS/GO/GCE is believed as an excellent electrode material for the sensing of dopamine.

1. INTRODUCTION

Dopamine (DA) is one of the catecholamine neurotransmitter which plays an important role in the central nervous system, circulatory system, and some other human physiological process [1]. DA functions as signal transmitter as well as it will control secretion level of sodium concentration on urine production in kidney [2]. Abnormal level of dopamine leads to causes several neurological related

diseases; for example, the high level of DA causes hungtington's diseases and reduce level leads to cause of Parkinson's and chronic renal parenchymal diseases [2]. Additionally, the imbalanced level of dopamine foremost reason for several health problems such as schizophrenia, hyperactivity, restless syndrome and HIV infection [3]. Therefore, the presence of dopamine in the living system is a significant essential factor for the clinical and recognition of diseases. Currently, no significant methods are available for the recording fluctuating level of DA in human sensory system. Various analytical techniques have been available for the detection of dopamine namely as spectrofluorometric [4], high-performance liquid chromatography [5], mass spectrometry [6], and electrochemical sensor [7]. As compared to traditional analytical methods, electrochemical methods are considered as a low-cost, very modest, and highly precise technique for the sensing of DA [8]. Further, DA is a redox molecule, electrochemical sensing based on its oxidation potential is a better choice for the quantitative detection of DA in human system [9]. However, the problem associated with the electrochemical detection of DA arises from the potential interfering compounds such as ascorbic and uric acid which are found high level in extracellular fluid of central nervous system which making it as tough enough to detect DA in human system [9]. Moreover, most of the electrodes are subject for fouling due to the significant adsorption of DA on the surface of the modified electrodes [10]. In order to overcome such problems, various nanomaterials such as carbon materials, conductive polymers, metal oxides, and metal sulfides has been developed. Introduction of various nanomaterials provide direct electrochemistry due to their direct high electron transfer rate and high conductivity [11]. Moreover, metal sulfides are low in cost, easy to prepare, semi conductive in nature [12]. Among the all, manganese sulfide (MnS) have received considerable response in the field of energy storage devices, dye sensitized solar cell, fuel cells and electrochemical sensor application [13–16]. Different metal sulfides with defined morphology namely CuS, NiS and MnS, have been developed and subjected for the electrochemical determination of biomolecules [17–19].

Apart from all other metal sulfides, Manganese sulfide (MnS) is known as a p-type semiconductor material and exists in different crystal structure form such as wurtz site and sphalerite. MnS exhibits an extraordinary electron transfer kinetics, high cyclic stability and low charge resistance leads to its high electrocatalytic activity [11]. Therefore, MnS based nanomaterials are widely used for various application such as optoelectronic devices, lithium-ion batteries and electrochemical sensor [20–22]. Besides, the electrochemical properties of Mn based compounds were improved by hybridizing with carbon nanomaterials [23]. Several carbon materials namely carbon nanofiber, graphene, carbon nanotube, and graphene oxide are available for the electrochemical sensing of biomolecules [24–27]. Among the all, graphene oxide is a well-known derivative of graphene, also have a large surface area, high electronic conductivity and mechanical strength due to the presence of a number of structural defects and functional groups (epoxy, hydroxyl, and carbonyl) on the plane [28]. Generally, highly functionalized graphene oxide shows large affinity toward metals or other species for electrochemical sensing of biomolecules [29]. In the past, N. Tukimin, introduced electrochemical deposited PEDOT/rGO/MnO$_2$ composite for electrochemical determination of uric acid, dopamine, and ascorbic acid [30]. Similarly, H.-L. Shuai, developed an microRNA sensor based on the manganese oxide/rGO/Au nanoparticles based on the enzyme amplification [31]. Based on the all aspects, we have

developed MnS decorated graphene oxide (MnS/GO) composite for the electrochemical sensing of dopamine.

In this work, we have synthesized and characterized MnS microspheres decorated graphene oxide (MnS/GO) composite by using simple hydrothermal method. Further the above prepared a composite were analyzed by using different techniques such as SEM, EDX, XRD and Raman Spectroscopy. Further, MnS/GO composite was used for electrochemical detection of dopamine. the electrochemical properties of MnS/GO modified electrode have been successfully reported by using Cyclic Voltammetry (CV), and linear sweep voltammetry (LSV) techniques. Remarkably, MnS/GO based reported sensor exhibits excellent electrochemical performance towards the detection of DA.

2. EXPERIMENT SECTION

2.1. Materials and reagents

The manganese chloride ($MnCl_2 \cdot 4H_2O$), thioacetamide (C_2H_5NS), dopamine were purchased from Sigma Aldrich. The hydrazine hydrate solution ($N_2H_4. xH_2O$) purchased from ACROS chemicals. $NaNO_3$ was purchased from Katayama Chemicals. H_2SO_4 (98%) were purchased from ACS reagent. The electrochemical behavior of MnS/GO was studied by using the supporting electrolyte 0.05 M phosphate buffer (PB) (pH 7) was prepared by using 0.05 M Na_2HPO_4 and NaH_2PO_4. The pH of the buffer was altered with the addition of $NaOH/H_2SO_4$.

2.2. Hydrothermal synthesis of MnS microspheres.

The MnS microspheres were prepared by simple hydrothermal method. In this experiment, 3.95 g of $MnCl_2. 4H_2O$ and 1.52 g of thioacetamide (C_2H_5NS) were mixed with 30 mL of DD water under continuous stirring for 1 hr. to the solution, about 10 ml of hydrazine hydrate solution were added and kept for magnetic stirring up to 2 hr. Afterwards, the resultant solution was transferred into 50 mL Teflon furnished auto clave and heated up to 180˚C for 24 hr in hot air oven. After that, the solution was kept for cooling under normal temperature. The obtained brown color precipitate was washed with ethanol and water up to several times and dried in vacuum oven at 45˚C for 24 hrs.

2.3. Preparation of MnS decorated Graphene oxide composite (MnS/GO)

Graphene oxide was prepared from the natural graphite powder by following the previously reported method [32]. In this synthesis, about 1 mg/mL of graphene oxide (GO) was dispersed in water by using ultrasonication process. After 15 min, the 5 mg of MnS powder was slowly added into the GO dispersion. Subsequently, the GO and MnS containing mixture was subjected to the ultrasonic treatment for 30 mins, while the reaction temperature was maintained at 50 °C. During the reaction time, homogenous (MnS/GO) suspension was turned into a dark black color which indicates the formation of

MnS microspheres decorated GO (MnS/GO) composite. Further, the above prepared composite was applied for electrochemical sensing of dopamine.

2.4. Characterization techniques

The surface morphology of as-synthesized MnS microspheres and MnS/GO composite were clearly confirmed by using SEM (Hitachi S-3000 H) analysis. Addtionally, the elemental distribution of as-synthesized MnS/GO was preliminarily studied by using Energy Dispersive X-ray spectroscopy (EDX, HORIBA EMAX X-ACT). The crystallographic nature of MnS/GO composite was studied through X-ray diffraction technique (XRD, XPERT-3 diffract meter with Cu Kα radiation (K= 1.54 Å)). the presence of defect site are confirmed by Raman analysis. Consequently, the electrochemical kinetics of MnS/GO/GCE towards the electrochemical detection of DA were studied by using CV and LSV(CHI611A) techniques. In this typical electrochemical experiment, the conventional three-electrode system was used, where the glassy carbon electrode (GCE) was used as a working electrode, a saturated Ag/AgCl electrode used as a reference electrode, and a platinum wire used as an auxiliary electrode. All electrochemical measurements were performed at room temperature.

2.5. Fabrication of MnS/GO/GCE

The electrode modification is an important process to record the true and reproducible electrochemical information of active material. In this modification process, MnS/GO nanocomposite (1 mg) was mixed with ehanol and kept for ultrasonuication upto 15 mins. Consequently, the prepared 6 μL of the MnS/GO suspension was drop cast on the surface of GCE and dried in air oven at 45℃. After drying, the modified MnS/GO was rinshed with DD water to remove the un bounded particles on GCE surface. Finally, the fabricated MnS/GO was used as a working electrode in all followed electrochemical studies. For the electrochemical application, the other modified electrodes such as MnS/GCE, GO/GCE, and bare GCE were fabricated by following the analogous process.

3. RESULTS AND DISCUSSION

3.1. Characterization of MnS microspheres and MnS/GO composite

The morphological studies were recorded for as prepared MnS and MnS/GO composite by using SEM analysis. **Fig. 1(A)** indicates SEM image of microsphere like structured MnS. Individual sheets of MnS particles are combined together to form microsphere like structure. Similarly, the morphology of MnS/GO composite were also estimated in **Fig. 1(B)** which gives clear evidence about the decoration MnS microspheres on the GO sheets. It was interesting to observe that the GO sheets are well covered and integrated by sphere-like structured MnS. The observed such type of GO integration can facilitate the more catalytic active sites to MnS and play a major role in electrochemical applications. Further stochiometric chemical composition of MnS/GO was estimated by using EDAX technique. The EDAX

spectra in **Fig. 1(C-D)**, gives details about the presence of constituent elements in MnS/GO composite such as manganese, sulfur, and carbon is along with elemental mapping shown in **Fig. 1(E-G)**.
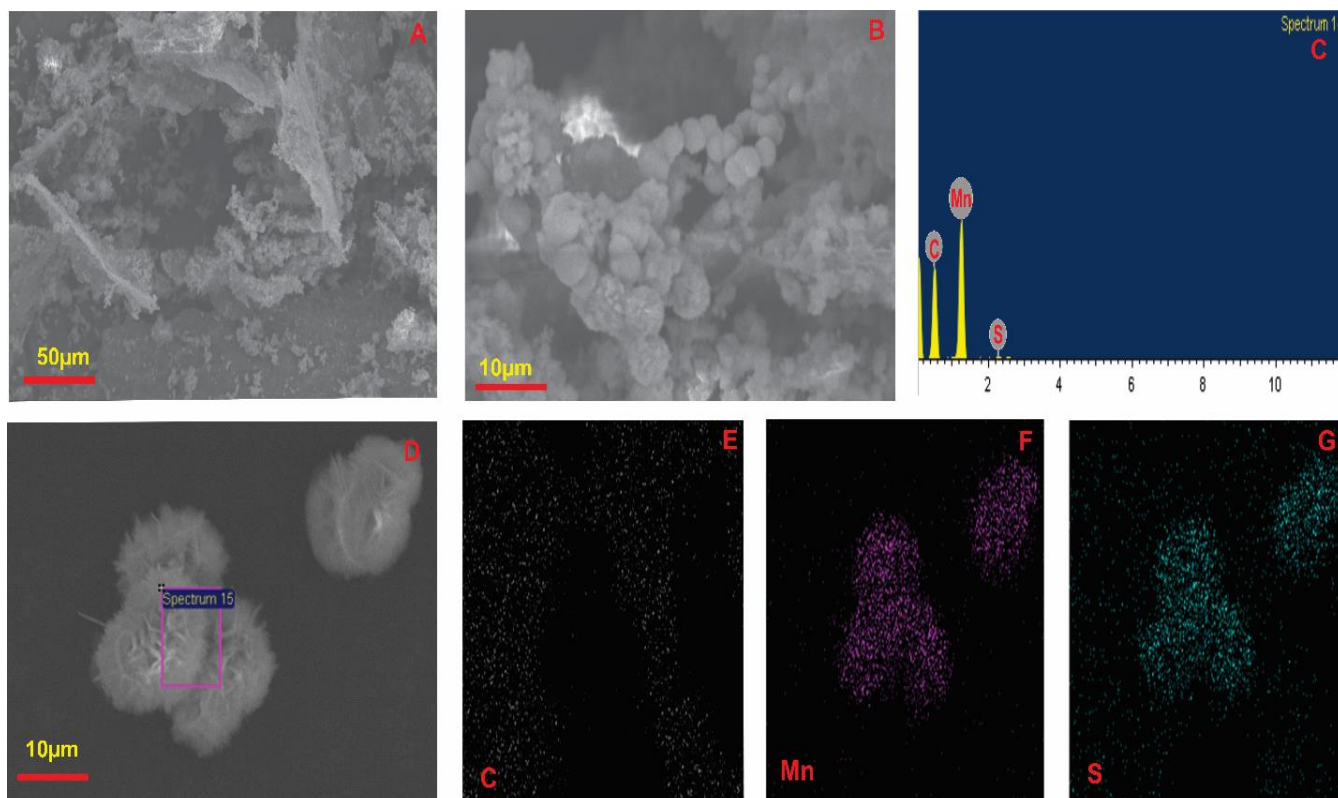

Figure 1. (A, B) SEM images of MnS/GO composite, (C) Corresponding EDAX spectrum of MnS/GO composite, (D) used for EDX analysis, (E-G) Element mapping images of MnS/GO composite.

Further, the crystalline nature of MnS microsphere and MnS/GO composite were analysed by using XRD. **Fig. 2(A,B)** indicates the XRD pattern of MnS microsphere and MnS/GO composite. The XRD pattern of MnS shows some diffraction peaks at 31.6º,34.4 º,44.9º,49.3º corresponding to the planes of (002), (101), (110), and (103). Similarly, MnS/GO shows diffraction peaks at 31.6º and 36.2º which are corresponding to the planes of (001), and (002) respectively. The all observed diffraction peaks are relatively can be supported to the tetragonal MnS phase with the cell parameter located at a = 5.22 Å, and C = 5.22 Å. The presence of GO was confirmed by change in the intensity of the diffraction peak corresponding to the MnS/GO composite. Besides, the obtained results are well matches with previous report data (JCPDS file:40-1289) [33]. Therefore, the formation of MnS/GO composite was confirmed by XRD analysis. Moreover, Raman spectra of MnS and GO gives additional evidence about ordered and disordered crystal structures of GO and which is shown in **Fig. 2(C)**. In these spectra, three major peaks were observed at 350.4, 650.4 cm^{-1}, corresponding to the non-stoichiometric ratio of MnS. The raman spectrum of GO shows characteristic G band and D band at 1357 and 1598 cm^{-1}. The G-band assigned to the band assigned to the E2g phonon mode of sp2-hybridized carbon atoms, and D-band assigned to the vibration of carbon atoms with dangling bonds in plane terminations of disordered

graphite. Further, the obtained peaks are well matching with the previously reported results of MnS and GO respectively [33].
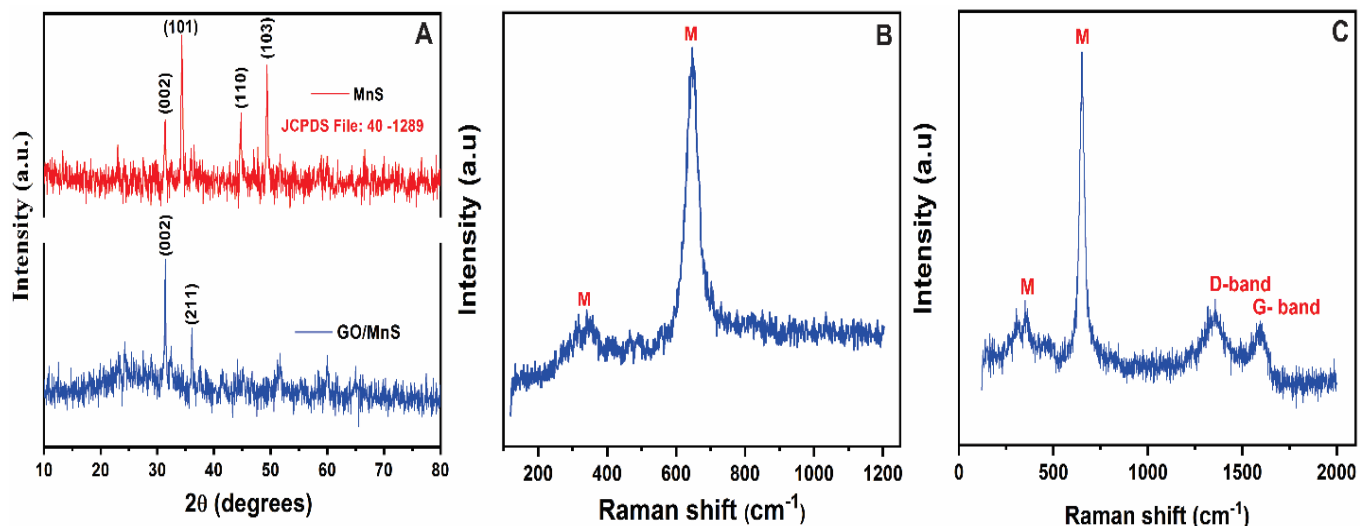

Figure 2. (A) XRD pattern and, RAMAN spectrum of (B) MnS and (C) MnS/GO composite

3.2. Electrochemical behavior of MnS/GO/GCE towards the electrochemical detection of DA

The electrochemical behavior of MnS/GO modified GCE were studied by using cyclic voltammetry. The CV results of MnS/GO/GCE was estimated in the presence of N_2 saturated 0.05 M PB (pH 7) at a scan rate of 50 mVs^{-1}. The corresponding CV curve of MnS/GO/GCE with the addition of 0.29 mM of DA shows high current response. The oxidation peak for DA on MnS/GO/GCE appears at a potential of 0.25 V and shown in **Fig. 3(A)**. while, MnS/GCE and GO/GCE exhibits a less intense current response towards determination of DA. but there is no significant peak response observed for bare GCE. Herein, the oxidation peak potential of DA was observed for MnS/GCE,GO/GCE and bare GCE of about 0.45, 0.31 and 0.51 V respectively. It clearly observed that the MnS/GO/GCE shows high peak response towards the detection of DA. Further, it is concluded that the MnS/GO/GCE is a highly suitable electrode for the determination of DA. Additionally, the electrochemical activity of MnS/GO/GCE was investigated in the presence of 0.05 M PB solution (pH 7) with the addition of different concentration of DA (0.09-0.921 mM) as shown in **Fig 3(B)**. The resultant CV curve indicates that the linear peak curernt increases with increase in concentration of DA from **Fig. 3(C).** Whereas, **Fig. 3(D)** indicates the corresponding linear curve for the peak current vs. concentration of DA with an calibration regression equation of y = -176.53x - 31.836 (y = I_{pa}(μA), x = DA), and a correlation coefficient of R^2 = 0.9912. Additionally, the linear curve for Log current vs log concentration of DA with a calibration regression equation of y = 0.7378x + 1.6694 and a correlation coefficient of R^2 = 0.898.
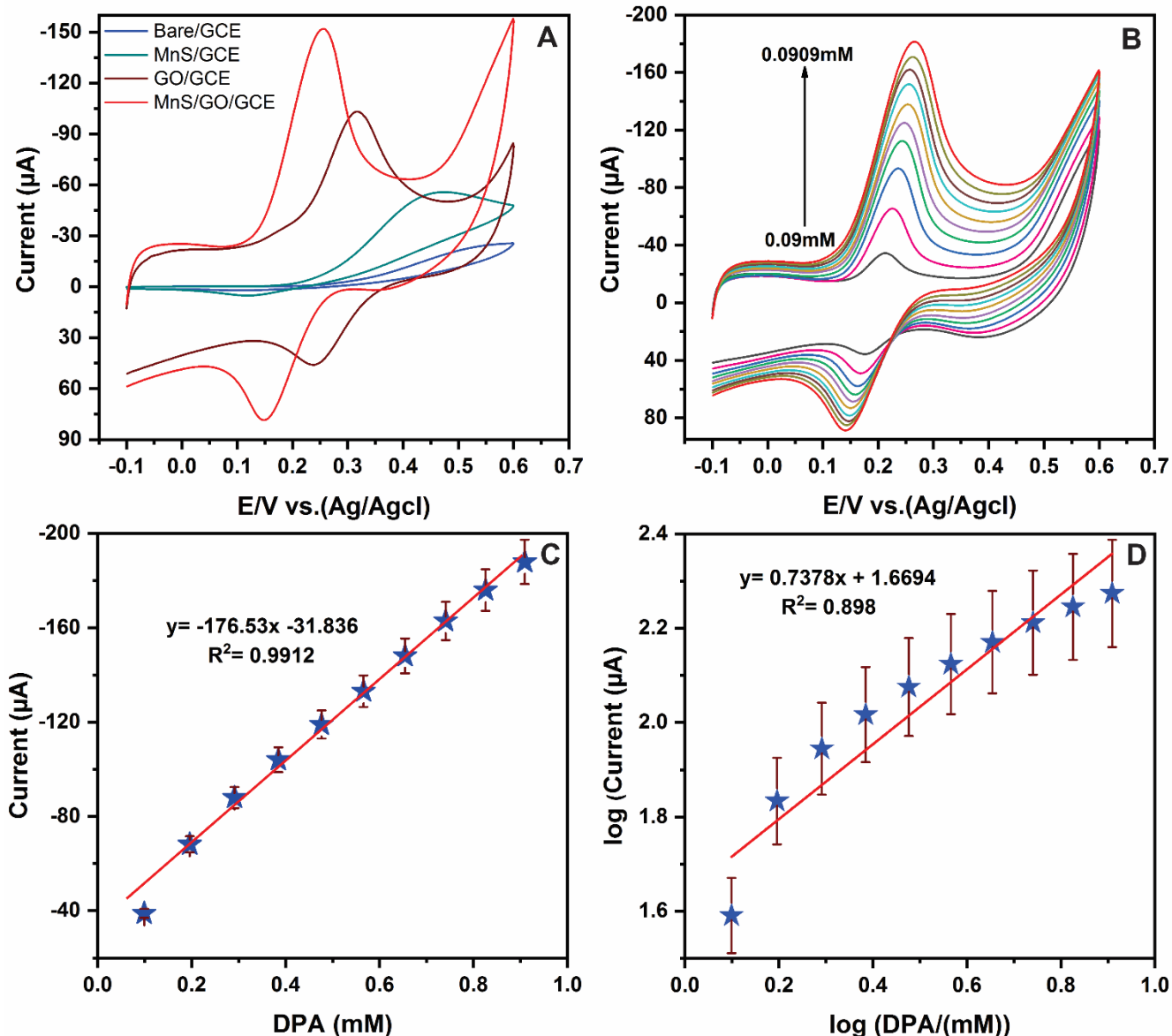
Figure 3. (A) Comparison (B) CV response of MnS/GO/GCE for variation in concentration of DA (0.09-0.909 mM) mM) in N_2 purged buffer (pH=7.0) at 50 mVs^{-1}. (C) Linear calibration plot for current Vs. concentration of DA (D) Log current vs log concentration of DA.

3.3. Effect of scan rate and pH for detection of DA at MnS/GO/GCE

The electrochemical behavior of modified electrode was affected by some important factors such as scan rate,pH of the electrolyte. The cyclic voltammetry experiment for oxidation of DA on MnS/GO/GCE was carried out in the presence of 0.05 M PB (pH 7) by varying scan rate from 10-100 mV s^{-1}. **Fig. 4(A)** indicates that the oxidation peak current of DA increases with increase in scan rate **[30]**. Additionally, the corresponding linear relationship between scan rate and current at the modified electrode is shown in linear plot **Fig. 4(B)**. from linear curve, the regression equation and correlation coefficient were calculated as y = -2.0604x – 39.695 (y = I_{pa}(μA), x = DA, and R^2 = 0.9954. Additionally, the resultant linear curve for peak current vs. log scan rate deduce that the linear regression and

correlation coefficients are y = 0.6627x + 1.0465 (y = $I_{pa}(\mu A)$, x = DA, and R^2 = 0.9969 respectively. It clearly implies that the electrochemical oxidation of DA at MnS/GO/GCE follows diffusion-controlled process.
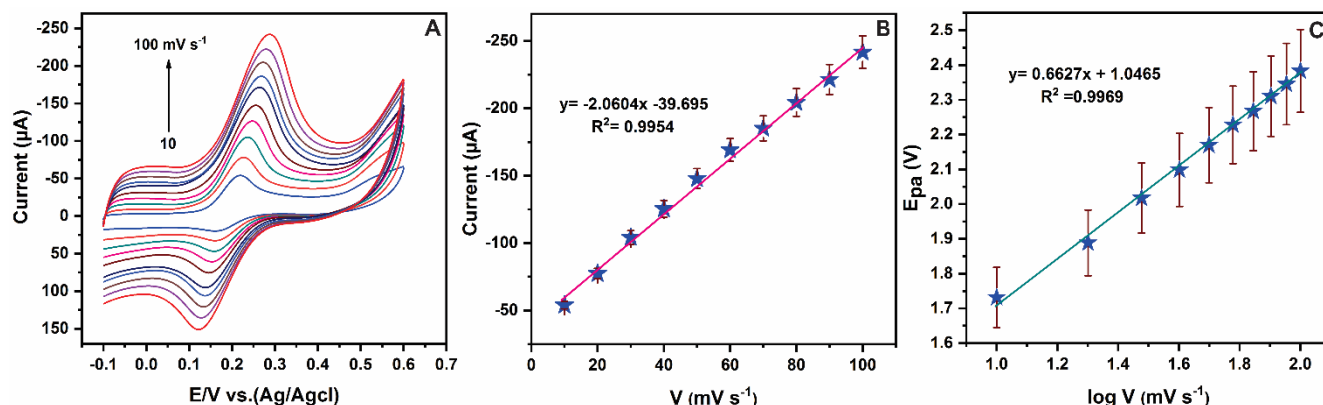

Figure 4. (A) CV response of MnS/GO/GCE scan rate (10- 100 mVs^{-1}) with in addition of DA (0.291 mM). (B) Linear curve for current Vs. scan rate (C) Corresponding calibration curve for current Vs. logarithm of scan rate.
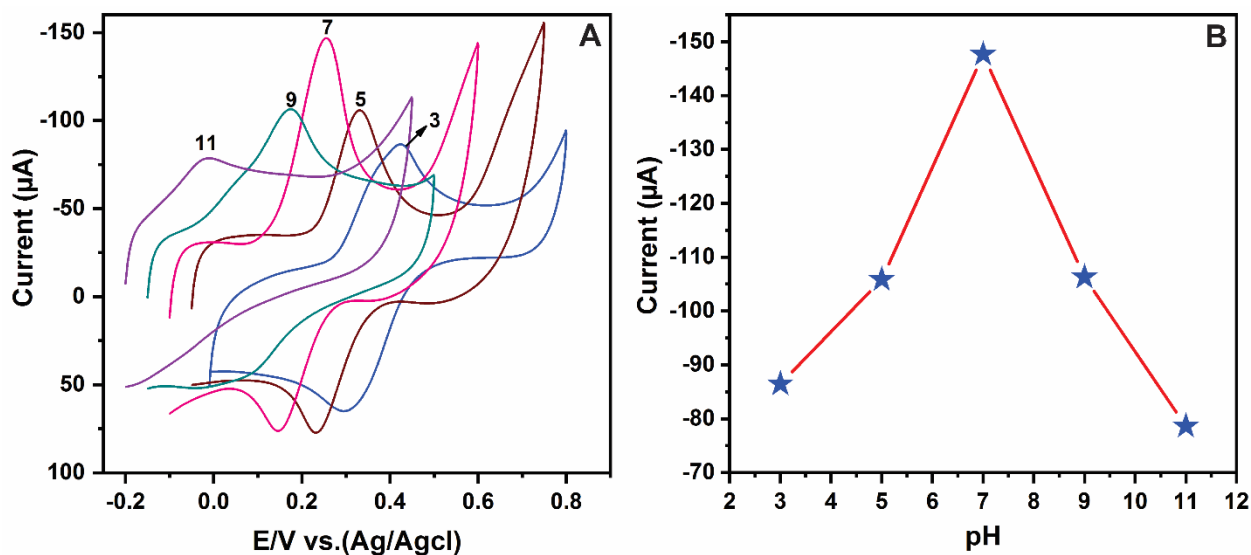

Figure 5. (A) CV response of MnS/GO/GCE for different pH (3 to 11) at scan rate of 50 mV/s^{-1} and (B) variation of anodic Peak current vs. pH.

In addition, the effect of pH on electrochemical behavior of DA at MnS/GO/GCE was estimated by using cyclic voltammetry by varying the pH range from 3 to 11. The CV experiment was performed in the presence of 0.05 M PB (pH 7) at a scan rate of 50 mV s^{-1}. The subsequent CV curve indicates anodic current increases while increasing pH from 3 to 7. Meanwhile, the anodic peak current decreased by increasing the pH from 7 to 11. The results are shown in **Fig 5(A)** and variation of anodic Peak current vs. pH indicated in **Fig 5(B)**. Finally, it was concluded that the pH 7 is an optimized pH level for the

electrochemical oxidation of DA. therefore, the buffer pH 7 was used for electrochemical oxidation of DA. Since the oxidation of dopamine to quinone form follows transfer of two number of electrons and protons in the redox process [7].

3.4. LSV technique for detection of DA at MnS/GO/GCE

The linear sweep voltammetry technique was used to investigate the electrocatalytic activity of MnS/GO/GCE towards the electrochemical oxidation of DA. The corresponding LSV curve was recorded and shown in **Fig. 6(A)** where the oxidation peak current increases with increasing the concentration of DA from 0.04-138.07 μM. In addition, the linear curve for peak current vs. DA concentration was shown in fig 6(B) with calibration regression equation and correlation coefficient of DA $y = -0.2286x – 7.4308$, $R^2 = 0.9927$, and $y = -0.0653x – 36.782$, $R^2 = 0.9951$ respectively. From the calibration plot, the detection limit of DA on MnS/GO/GCE calculated by the using equation,

$$LOD = 3\sigma/S \quad (1)$$

Herein, σ is the standard deviation of the blank signal and S is the slope of the calibration curve. the detection limit and sensitivity of DA on MnS/GO/GCE were calculated to be 0.007 μM and 3.11 μA μM^{-1}cm^{-2} respectively. To understand the improvement of the reported sensor, the calculated detection limit and sensitivity were compared with previously reported DA sensors as shown in **Table (1)**.

Table 1. Comparison of MnS/GO/GCE modified electrode with recently reported on electrochemical sensing of DA.

Electrode type	Technique	Linear range (μM)	Detection limit (μM)	References
NP-PtY/GR/GCE	DPV	0.9-82	0.36	[34]
p-GLY/GO/GCE	DPV	0.20-62	0.011	[35]
3D HGBs/ITO electrode	DPV	1-60	1	[36]
AG-NA/GCE	DPV	0.5-35	0.33	[37]
RGO-TiN/GCE	DPV	1-80	1	[38]
LiMn Po$_4$/f-MWCNT/GCE	DPV	0.1-49	0.019	[39]
ZnO/Al$_2$O$_3$	DPV	5.0-700.0	2.0	[40]
Pt/CNT/GR/GCE	DPV	0.01-30	0.01	[41]
GQDs/GCE	DPV	0.4-100	0.05	[42]
MWCNT/GCE	DPV	5-50	0.33	[43]
MnS/GO/GCE	LSV	0.04-138.07	0.007	This work

3.5. Selectivity and Stability studies on MnS/GO/GCE towards the detection of DA

In general, the practicability of an electrochemical sensor was defined from some factors like selectivity and stability tests. Thus, the reported sensor was treated with the following electrochemical experiments to determine these important factors. To understand the selectivity of MnS/GO/GCE, the LSV was performed at MnS/GO/GCE, with presence of DA (0.291 mM) and the addition of 100-fold

higher concentration of interference species such as organic species such as dopamine (DA), ascorbic acid (AA), uric acid (UA), hydroquinone (HQ), glucose, catechol (CT) and some metal ions (Zn^{2+}, Cu^{2+}, Fe^{2+} and Co^{2+}). The obtained LSV curve is shown in the **Fig. 6(C)**, and the corresponding bar diagram for relative error (%) also given in **Fig. 6(D).** From the results, the negligible amount of response only observed for the addition of interference species. It reveals that the feasible selectivity of the MnS/GO/GCE modified electrochemical sensor, similarly, cyclic stability of the MnS/GO/GCE was studied by using LSV in the presence of DA (50 cycles) and which is shown in **Fig. 7(A).** Therefore, it is concluded that the MnS/GO/GCE sensor exhibits excellent storage stability.
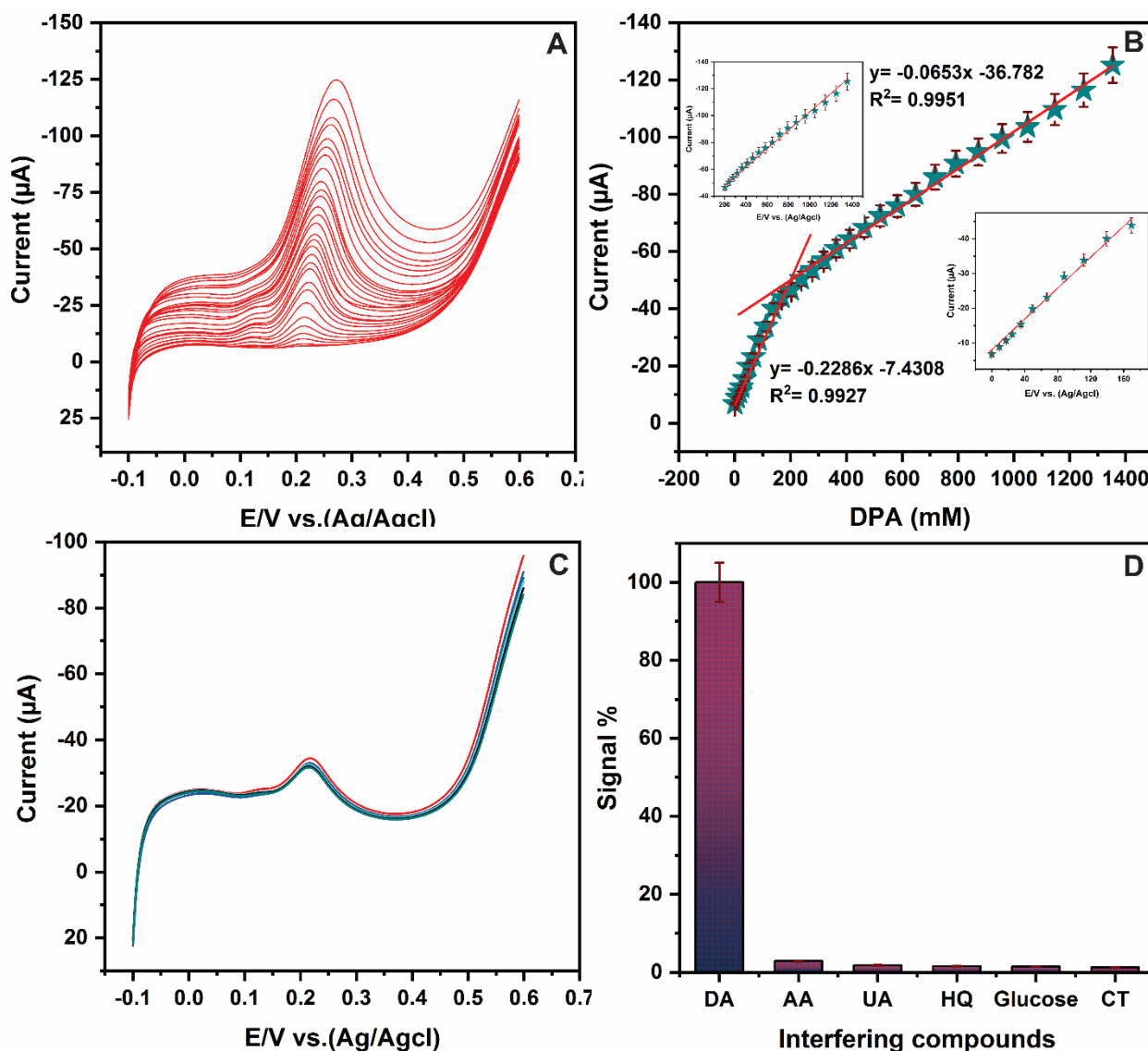

Figure 6. (A) LSV response of MnS/GO/GCE for continuous addition DA from (0.04-138.07 μM) in 0.05M PB solution (pH=7). (B) The calibration plot of anodic peak current vs. Concentration of DA. (C) The LSV responses for Interfering compounds (D) error bar diagram for interfering species in LSV.

3.6. Real sample analysis

Real sample analysis of MnS/GO/GCE was carried out in the presence of human urine samples. For this experiment, a known concentration of DA from human urine sample was spiked into the PBS (pH 7) solution. Further, the LSV result of MnS/GO/GCE was estimated for the addition of DA spiked human urine sample. The probable recovery values are ranging from 101.1 to 107.5 % for DA respectively. The obtained recovery results are summarized in **Table (2)**. The estimated result in real sample test recommended that the outstanding practicability of MnS/GO/GCE toward the detection of DA in human urine sample.
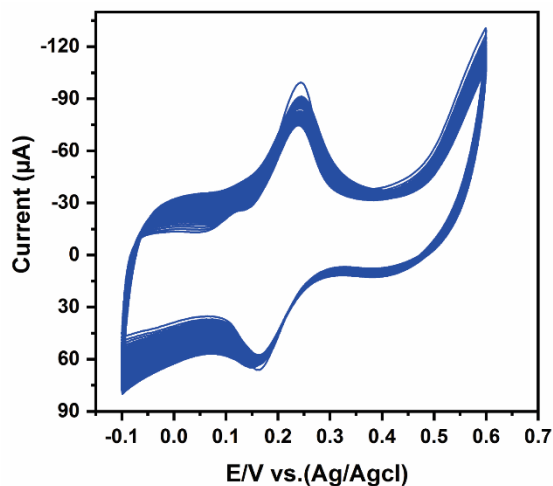

Figure 7. (A) The DPA response of cyclic stability test (50 cycle) of MnS/GO/GCE in N_2 saturated 0.05M PB solution (pH7).

Table 2. Detection of DA in human urine sample at MnS/GO/GCE (n = 4)

Sample	Added (µM)	Found (µM)	Recovery (%)	RSD (%)
Urine	0	Not found	Not found	Not found
	2	2.1	105	2.3
	4	4.3	107.5	2.3
	6	6.2	103.3	2.4
	8	8.1	101.2	2.5

4. CONCLUSION

In the present work, we have prepared MnS/GO/GCE composite by using a facile hydrothermal method and analyzed by using different methods such as SEM, EDX, XRD, and Raman. The proposed MnS/GO/GCE exhibits high catalytic activity and used for electrochemical detection of DA. Further, MnS/GO/GCE shows high electrical conductivity as compared to previous reported sensor. As expected, MnS/GO/GCE exhibited high electrocatalytic activity towards the detection of DA with an ultra-low

detection limit (0.007µM) sensitivity (3.11 µA µM^{-1}cm^{-2}). Finally, we are successfully reported the feasible selectivity, storage stability and reproducibility of the proposed sensor which is more advantages for the excellent practicability of MnS/GO/GCE to determine DA in human urine sample.

NOTES
The authors declare no competing financial interest

References

1. K.S. Ahmad, Z. Hussain and S. Majid, *Surfaces and Interfaces*, 12 (2018) 190.
2. S.K. Shukla, A. Lavon, O. Shmulevich and H. Ben-yoav, *Talanta,* 181 (2018) 57.
3. M. Singh, I. Tiwari, C.W. Foster and C.E. Banks, *Materials Research Bulletin,* 101 (2018) 253.
4. W. Wei, H.J Wang and C.Q jiang, *The journal of biological and chemical luminescence*, 22 (2007) 581.
5. N. Ye, T. Gao and J. Li, *Anal. Methods,* 6 (2014) 7518.
6. A. El-beqqali, A. Kussak and M. Abdel-rehim, *J. Sep. Sci,* 33 (2007) 421.
7. D. Thirumalai, D. Subramani, J. Yoon, J. Lee, H. Paik and S. Chang, *J. Chem.,* 42 (2018) 2432.
8. Y.V. Manohara, B. Sravani, S. Agarwal and V. Kumar, *J. Electroanal. Chem.,* 820 (2018) 168.
9. L.A. Mercante, A. Pavinatto, L.E.O. Iwaki, V.P. Scagion, V. Zucolotto, O.N. Oliveira, L.H.C. Mattoso and D.S. Correa. *ACS Appl. Mater. Interfaces,* 7 (2015) 4784.
10. J. Huang, Y. Liu, H. Hou and T. You, *Biosens. Bioelectron.,* 24 (2008) 632.
11. S. He, W. Qiu, L. Wang, F. Gao, W. Wang, Z. Hu and Q. Wang, *J. Mater. Sci.,* 51 (2016) 7156.
12. H.R. Zare-mehrjardi, *Quarterly Iranian Chemical Communication,* 6 (2018) 300.

13. V.A. Online, X. Rui and Q. Yan, *Nanoscale,* 6 (2014) 9889.
14. J. Luo, Y. Xiang, J. Sun, Z. Sheng and Q. Feng, *Sol. Energy Mater. Sol. Cells,* 187 (2018) 199.
15. A. Asokan and P. Shaik, 10.1002/celc.201700160.
16. S.C. Riha, A.A. Koegel, X. Meng, I.S. Kim, Y. Cao, M.J. Pellin, W. Elam, and A.B.F. Martinson, *ACS Appl. Mater. Interfaces,* 8 (2016) 2774.
17. Y.J. Yang, W. Li and X. Wu, *Electrochim. Acta,* 123 (2014) 260.
18. J. Zhang, C. Xu, D. Zhang, J. Zhao, S. Zheng, H. Su, F. Wei, B. Yuan, and C. Fernandez, *J. Electrochem. Soc.,* 164 (2017) B92.
19. Y. Gong, and Z. Fan, *Sensors Actuators, B Chem.*, 202 (2014) 638.
20. B. Ghanbari, F. Jamali and S. Ramin, *J. Mater. Sci. Mater. Electron.,* 29 (2018) 10976.
21. Y. Hao, C. Chen, X. Yang, G. Xiao, B. Zou, J. Yang and C. Wang, *J. Power Sources,* 338 (2017) 9.
22. C. Cheng, D. Kong, C. Wei, W. Du, J. Zhao, Y. Feng and Q. Duan, *Dalton Transaction,* 46(2017) 5406.
23. X. Zhang, P. He, X. Zhang, C. Li and H. Liu, *Electrochim. Acta.* 276 (2018) 92.
24. M. Sakthivel, S. Ramaraj, C. Shen-ming, B. Dinesh and C. Kuang-hsiang, *J. Taiwan Inst. Chem, Eng.,* 000 (2017) 1.
25. J.S. Kumar, N.C. Murmu and T. Kuila, 5 (2018) 422–466. doi:10.3934/matersci.2018.3.422.
26. A.J.S. Ahammad, T. Akter, A. Al Mamun, T. Islam, M. Hasan, M.A. Mamun, S. Faraezi, F.Z. Monira and J.K. Saha, *Journal of The Electrochemical Society,* 165 (2018) B390.

27. Q. He, J. Liu, X. Liu, Y. Xia, G. Li and P. Deng, *Molecules,* 23 (2018) 2130.
28. S. Azizighannad and S. Mitra, *Sci. Rep.*, (2018) 1.
29. J. Li, D. Kuang, Y. Feng, F. Zhang, Z. Xu and M. Liu, *J. Hazard. Mater.,* 201(2012) 250.
30. N. Tukimin, J. Abdullah and Y. Sulaiman, *J. Electroanal. Chem.,* 820 (2018) 74.
31. H. Shuai, K. Huang, W. Zhang, X. Cao and M.P Jia, *Sensors and Actuators B: Chemical,* 243 (2017) 403.
32. X. Zhang, H. Wang, T. Huang, L. Wen and L. Zhou, *Materials Research Express,* 5 (2018) 035515.
33. J. Beltran-Huarac, J. Palomino, O. Resto, J. Wang, W.M. Jadwisienczak, B.R. Weiner, and G. Morell, *RSC Adv.*, 4 (2014) 38103.
34. Y. Haldorai, A.T.E. Vilian, M. Rethinasabapathy, Y.S. Huh and Y.K. Han, *Sensors Actuators, B Chem.,* 247 (2017) 61.
35. S. He, P. He, X. Zhang, X. Zhang, K. Liu, L. Jia and F. Dong, *Anal. Chim. Acta,* 1031 (2018) 75.
36. H.Y. Yue, S.S. Song, S. Huang, X. Gao, B. Wang, E.H. Guan, H.J. Zhang, P.F. Wu and X.R. Guo, *J. Mater. Sci. Mater. Electron.,* 29 (2018) 12330.
37. D. Kim, S. Lee and Y. Piao, *J. Electroanal. Chem.,* 794 (2017) 221.
38. Y. Haldorai, A.T.E. Vilian, M. Rethinasabapathy, Y.S. Huh and Y.-K. Han, *Sensors Actuators B Chem.*, 247 (2017) 61.
39. N. Raja, and Shen-Ming Chen. *RSC Advances,* 8(49) (2018) 27775.
40. M.R. Ganjali, H. Beitollahi, R. Zaimbashi, S.Tajik, M. Rezapour and B. Larijani. *Int. J. Electrochem. Sci.,* 13 (2018) 2519.
41. S. Ramakrishnan, K.R. Pradeep, A. Raghul, R. Senthilkumar, M Rangarajan and N. K. Kothurkar. *Analytical Methods,* 7 (2015) 779.
42. S. Zheng, R. Huang, X. Ma, J. Tang, Z. Li, X. Wang, J. Wei and J. Wang, *Int. J. Electrochem. Sci*, 13 (2018) 5723
43. B.Habibi and M.H Pournaghi-Azar, *Electrochimica Acta*, *55 (*2010) 5492.